THE COMPUTATION OF DISCONNECTED BIFURCATION DIAGRAMS

P. E. FARRELL*, C. H. L. BEENTJES[†], AND Á. BIRKISSON[‡]

Abstract. Arclength continuation and branch switching are enormously successful algorithms for the computation of bifurcation diagrams. Nevertheless, their combination suffers from three significant disadvantages. The first is that they attempt to compute only the part of the diagram that is continuously connected to the initial data; disconnected branches are overlooked. The second is that the subproblems required (typically determinant calculation and nullspace construction) are expensive and hard to scale to very large discretizations. The third is that they can miss connected branches associated with nonsimple bifurcations, such as when an eigenvalue of even multiplicity crosses the origin. Without expert knowledge or lucky guesses, these techniques alone can paint an incomplete picture of the dynamics of a system.

In this paper we propose a new algorithm for computing bifurcation diagrams, called deflated continuation, that is capable of overcoming all three of these disadvantages. The algorithm combines classical continuation with a deflation technique that elegantly eliminates known branches from consideration, allowing the discovery of disconnected branches with Newton's method. Deflated continuation does not rely on any device for detecting bifurcations and does not involve computing eigendecompositions; all subproblems required in deflated continuation can be solved efficiently if a good preconditioner is available for the underlying nonlinear problem. We prove sufficient conditions for the convergence of Newton's method to multiple solutions from the same initial guess, providing insight into which unknown branches will be discovered. We illustrate the success of the method on several examples where standard techniques fail.

Key words. continuation, bifurcation, deflation, branch switching, deflated continuation.

AMS subject classifications. 65P30, 65L10, 65L20, 65H10.

1. Introduction. We consider numerical methods for computing the solutions of

$$f(u,\lambda) = 0, (1.1)$$

where $f: U \times \mathbb{R} \to Y$ is the C^1 problem residual, U and Y are isomorphic Banach spaces, $u \in U$ is referred to as the solution, and $\lambda \in \mathbb{R}$ is referred to as the parameter. In our applications, (1.1) typically represents the residual of a stationary ordinary or partial differential equation, along with boundary conditions. The associated bifurcation diagram visualizes how the behaviour of a functional of the solutions changes as λ is varied over some interval of interest $[\lambda_{\min}, \lambda_{\max}]$.

Arclength continuation and branch switching [17, 10, 15, 8, 27] are central techniques in the computational analysis of (1.1) and are routinely used throughout science and engineering. Given an initial point (u_0, λ_0) on a branch, arclength continuation (or its popular variant, pseudo-arclength continuation) robustly traces out the remainder of that branch. It parameterizes the solution and parameter $(u(s), \lambda(s))$ as

^{*}Mathematical Institute, University of Oxford, Oxford, UK. Center for Biomedical Computing, Simula Research Laboratory, Oslo, Norway (patrick.farrell@maths.ox.ac.uk).

 $^{^\}dagger Mathematical\ Institute,\ University\ of\ Oxford,\ Oxford,\ UK\ (\texttt{beentjes@maths.ox.ac.uk}).$

[‡]Mathematical Institute, University of Oxford, Oxford, UK (birkisson@maths.ox.ac.uk). This research is funded by EPSRC grants EP/K030930/1 and EP/M019721/1, by a Clarendon Fund Scholarship, by a New College Graduate Scholarship, by the European Research Council under the European Union's Seventh Framework Programme (FP7/2007-2013)/ERC grant 291068, and by a Center of Excellence grant from the Research Council of Norway to the Center for Biomedical Computing at Simula Research Laboratory. The authors would like to thank L. N. Trefethen for useful discussions and G. N. Wells for furnishing the hyperelastic solver used in section 4.4.

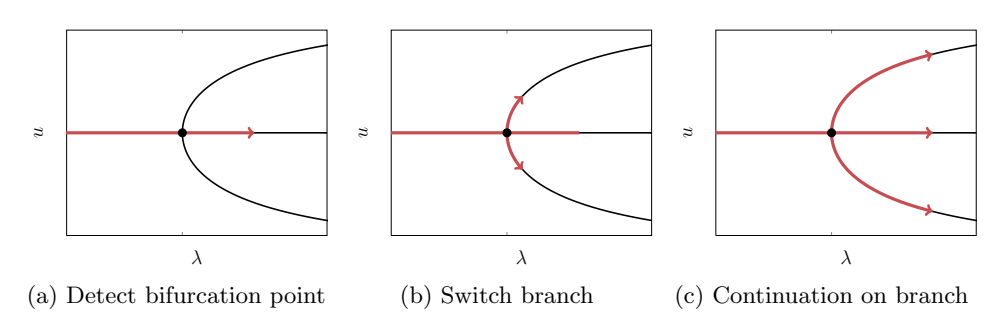


Fig. 1.1: Sketch of switching continuation. Arclength (or pseudo-arclength) continuation is applied on a branch as in Figure 1.1a. When a bifurcation point is detected, the nullspace of the Fréchet derivative there is computed and is used to switch branch, depicted in Figure 1.1b. Once a point on the emanating branch is known, continuation traces out the branch as in Figure 1.1c.

a function of arclength along the curve s from the initial point, as this allows the method to continue through fold bifurcations. It applies a predictor computed from previous solutions to estimate the solution and parameter for $s + \Delta s$, and corrects this guess with a solver such as Newton's method.

Branch switching algorithms attempt to detect bifurcation points along a branch and to construct initial solutions on the branches emanating from it, Figure 1.1. The detection step typically relies on the computation of the bifurcation test functional

$$\tau(u,\lambda) = \operatorname{sign}(\det J(u,\lambda)) = \operatorname{sign}\left(\prod_{i} \mu_{i}(u,\lambda)\right),$$
(1.2)

where μ_i are the eigenvalues of the (discretized) Jacobian J, including multiplicities. This test functional is cheaply computable if an LU decomposition of J is already available from a continuation step [27], but is very difficult to estimate if a Krylov method is used. Once a bifurcation point has been identified, initial guesses for solutions on the emanating branches are constructed from the nullspace of J there. Once one solution on each emanating branch is known, arclength continuation is used to complete the branch. Henceforth, this combination of arclength continuation and branch switching will be referred to as *switching continuation*.

Switching continuation computes fragments of bifurcation diagrams: it attempts to compute the part of the bifurcation diagram that is continuously connected to the initial point (u_0, λ_0) . However, it is often the case that the bifurcation diagram is not connected, with multiple branches that do not meet at bifurcation points. For example, pitchfork and transcritical bifurcations are not generic; they are destroyed under perturbation [15, Chapter IV], and subsequently the complete bifurcation diagram cannot be computed in one pass with the approach described above. Other examples will be given in section 4. In these cases, the diagram returned by switching continuation along a single path is incomplete, giving an unsatisfactory picture of the solutions to (1.1).

In this work we develop and analyze an alternative algorithm, deflated continuation, that is capable of discovering disconnected branches from known ones, without

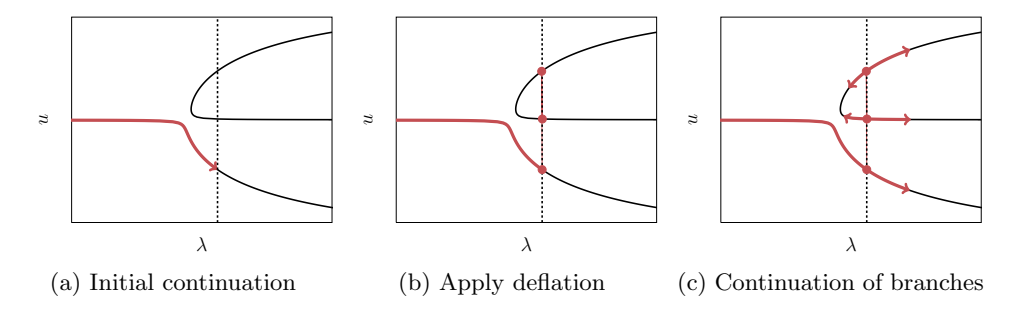


Fig. 1.2: Sketch of deflated continuation, the algorithm proposed in this work. Continuation is applied on a branch as in Figure 1.2a. Along the branch, we stop and fix the parameter λ , then attempt a deflation step to find multiple solutions for this parameter as in Figure 1.2b. If the deflation step is successful, we have points on multiple branches and can continue these branches as in Figure 1.2c.

requiring that a bifurcation point connect the two, Figure 1.2. At the heart of the method is the deflation of known solutions [7, 14]. Deflation is a technique that systematically modifies a nonlinear problem to guarantee that Newton's method will not converge to a known root, thus enabling unknown roots to be discovered from the same initial guess. Fix λ in (1.1) to yield the nonlinear problem

$$F(u) = 0, (1.3)$$

where $F: U \to Y$. Suppose Newton's method is applied to F from initial guess u_0 to yield the solution u_1^* , with the Fréchet derivative $F'(u_1^*)$ nonsingular. Suppose further that we suspect that (1.3) permits solutions other than u_1^* , but no additional initial guesses are available. We thus construct a modified problem

$$G(u) = M(u; u_1^*)F(u),$$
 (1.4)

via the application of a deflation operator $M(u; u_1^*)$ to the residual F. By construction, this deflated residual satisfies two properties. The first is the preservation of solutions of F, i.e. for $u \neq u_1^*$, G(u) = 0 iff F(u) = 0. The second is that Newton's method applied to G will not discover u_1^* again, as

$$\liminf_{u \to u_1^*} \|G(u)\| > 0,$$
(1.5)

i.e. along any sequence converging to the known root, the deflated residual does not converge to zero. Thus, if Newton's method applied to G converges from u_0 , it will converge to a distinct solution $u_2^* \neq u_1^*$. The process can then be repeated until no more solutions are found from u_0 in a specified number of Newton iterations. In this work, we use the shifted deflation operator

$$M(u; u_1^*) = \left(\frac{1}{\|u - u_1^*\|^p} + \sigma\right) \mathbb{I},\tag{1.6}$$

where \mathbb{I} is the identity on Y, p is the power, and σ is the shift. All of the examples below use p=2 and $\sigma=1$. Importantly, it is possible to efficiently solve the Newton

step for G if a good preconditioner is available for the Newton step of F. For more details, see [1, 14, 13].

We present the proposed bifurcation algorithm in section 2. To analyze its behaviour, in section 3 we develop an initial theory of *multiconvergence* of Newton's method. We derive novel sufficient conditions under which Newton's method will converge to two different solutions, starting from the same initial guess. In section 4, the method is applied to several problems on which switching continuation fails.

Algorithm 2.1. Deflated continuation.

```
Input: Initial parameter value \lambda_{\min}.
Input: Final parameter value \lambda_{\text{max}} > \lambda_{\text{min}}.
Input: Step size \Delta \lambda > 0.
Input: Nonlinear residual f(u, \lambda).
Input: Deflation operator M(u; u^*).
Input: Initial solutions S(\lambda_{\min}) to f(\cdot, \lambda_{\min}).
 1: \lambda \leftarrow \lambda_{\min}
 2: while \lambda < \lambda_{\max} do
           F(\cdot) \leftarrow f(\cdot, \lambda + \Delta\lambda)
                                                                               \triangleright Fix the value of \lambda to solve for.
           S(\lambda + \Delta \lambda) \leftarrow \varnothing
  4:
           for u_0 \in S(\lambda) do
                                                                                      ▷ Continue known branches.
  5:
                apply Newton's method to F from initial guess u_0.
  6:
  7:
                if solution u^* found then
                     S(\lambda + \Delta \lambda) \leftarrow S(\lambda + \Delta \lambda) \cup \{u^*\}
                                                                                                     \triangleright Record solution.
  8:
                     F(\cdot) \leftarrow M(\cdot; u^*)F(\cdot)
                                                                                                     ▷ Deflate solution.
 9:
           for u_0 \in S(\lambda) do
                                                                                                 ▷ Seek new branches.
10:
                success \leftarrow true
11:
                while success do
12:
                     apply Newton's method to F from initial guess u_0.
13:
                     if solution u^* found then
                                                                                                 ▶ New branch found.
14:
15:
                           S(\lambda + \Delta \lambda) \leftarrow S(\lambda + \Delta \lambda) \cup \{u^*\}
                                                                                                     \triangleright Record solution.
16:
                           F(\cdot) \leftarrow M(\cdot; u^*)F(\cdot)
                                                                                                     ▶ Deflate solution.
                     else
17:
                          success \leftarrow false
18:
           \lambda \leftarrow \lambda + \Delta \lambda
19:
20: \mathbf{return} \ S
```

2. Deflated continuation. Let $[\lambda_{\min}, \lambda_{\max}]$ be the interval of interest for the parameter λ , and let $\Delta\lambda$ be the continuation step size. For a given λ , let $S(\lambda) \subset U$ denote the set of known solutions to (1.3). Given $S(\lambda)$, Algorithm 2.1 constructs $S(\lambda + \Delta\lambda)$ as follows. In the first pass (lines 5–9), known solutions are continued with standard classical continuation; each known solution $u_0 \in S(\lambda)$ is used as initial guess for $f(\cdot, \lambda + \Delta\lambda)$ in turn. If some solutions are not successfully continued, the algorithm proceeds with the other branches regardless. (This can happen at fold bifurcations, for example.) As each solution is continued, it is recorded and deflated. In the second pass (lines 10–18), each initial guess is again considered in turn. Deflation guarantees that Newton's method will not return to the known branch, and hence if Newton's method converges, it will converge to a previously unknown solution (line 14). Each initial

guess is attempted repeatedly until no solution is found within a certain number of Newton iterations. (Recall that Newton's method is undecidable, i.e. it is impossible to decide in general if Newton's method will eventually converge for a given initial guess [6].) Once all initial guesses have been exhausted, the algorithm increments λ and continues until the end of the interval has been reached.

2.1. Variants of the algorithm. Various modifications to the basic algorithm are possible. The analyst may decide to seek unknown branches with a step size larger than $\Delta\lambda$, to reduce the effort spent on unsuccessful Newton iterations. The continuation and discovery stages are independent and may be executed in parallel; one group of processors can continue known solutions forwards, while other groups follow behind, seeking new solutions to continue.

If the system (1.1) has a finite symmetry group \mathcal{G} such that for all $g \in \mathcal{G}$,

$$f(u,\lambda) = 0 \iff f(gu,\lambda) = 0,$$
 (2.1)

then when a solution u is discovered, its actions $\mathcal{G}u$ should be recorded and deflated as well, assuming that it is possible to represent each gu exactly with the discretization employed. If the discretization does not respect this symmetry (e.g. a finite element discretization on an unstructured mesh), then the projection of gu should be used as initial guess for Newton's method instead. Deflating infinite symmetry groups will be studied in future research.

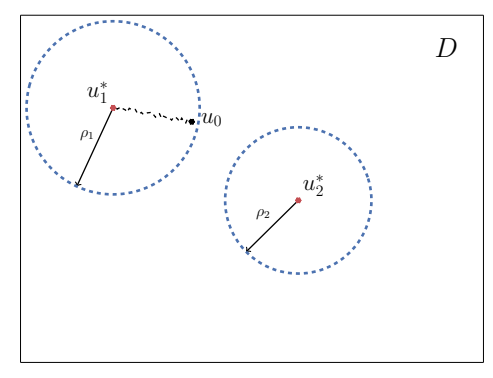
If the system (1.1) has a trivial branch \bar{u} such that $f(\bar{u}, \lambda) = 0$ for all λ , then this branch must be excluded from the set of initial guesses to use in deflation. This is because the initial residual of (1.4) will evaluate to 0/0. As such trivial branches are obvious from the equations, the simplest approach is just to deflate any trivial solutions away before beginning Algorithm 2.1.

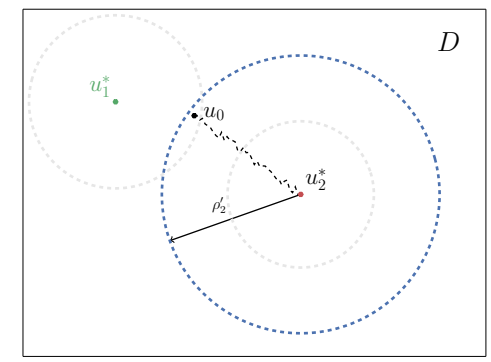
In the discovery stage, problem-specific guesses other than the previous solutions may be employed; for example, in nonlinear eigenproblems it may be useful to use the eigenmodes of an associated linear problem. It may be necessary to break the symmetry of the guesses: if the system (1.1) has a \mathbb{Z}_2 symmetry R such that $f(Ru,\lambda) = Rf(u,\lambda)$, then if Newton's method is initialized with a symmetric initial guess satisfying $Ru_0 = u_0$ then all subsequent iterates will also remain symmetric. This will cause nonconvergence to nonsymmetric solutions, such as those introduced at a symmetry-breaking bifurcation. In this regard it may be advantageous to deliberately break the symmetry of the discretization, or if this is not possible (such as when using a spectral method), to deliberately break the symmetry of the initial guesses.

It is straightforward in principle to employ other continuation approaches in Algorithm 2.1: if arclength continuation is used, then in the first pass each branch is synchronized at $\lambda + \Delta \lambda$, deflation is applied to seek new branches, and the process is repeated.

3. Convergence analysis. The central question in the analysis of Algorithm 2.1 is: under what circumstances will unknown branches be discovered, and under what circumstances will they be missed? Given an initial guess u_0 , we wish to derive sufficient conditions that guarantee convergence to at least two solutions u_1^* and u_2^* with Newton's method and deflation, Figure 3.1. In the context of Algorithm 2.1, u_0 is the known solution for $f(\cdot, \lambda)$, u_1^* is the solution on the same branch for $f(\cdot, \lambda + \Delta \lambda)$, and u_2^* is another solution to $f(\cdot, \lambda + \Delta \lambda)$ on a different branch.

The best-known theorem of convergence for Newton's method is the theorem of Kantorovich [16], who first formulated and analyzed Newton's method in Banach





- (a) Convergence before deflation
- (b) Convergence after deflation

Fig. 3.1: Sketch of the regions of convergence around solutions u_1^* and u_2^* before and after deflation. Before deflation, the initial guess u_0 converges to u_1^* ; after deflating this solution, the region of convergence around u_2^* expands and u_0 now lies within it.

spaces. We state the theorem (and all subsequent results) in affine-covariant form [9].

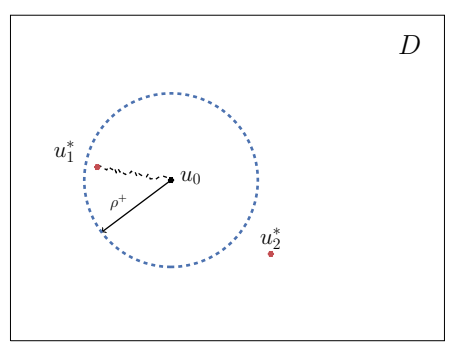
THEOREM 3.1 (Affine-covariant Newton-Kantorovich [16]). Let $F: D \to Y$ be a continuously Fréchet differentiable function on the open convex subset $D \subseteq U$. Given $u_0 \in D$, assume that

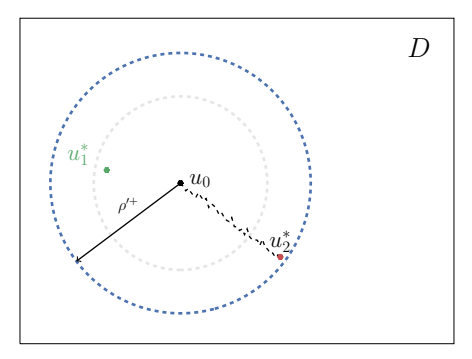
- i) $F'(u_0)^{-1}$ exists; let $\alpha = ||F'(u_0)^{-1}F(u_0)||$;
- *ii)* $||F'(u_0)^{-1}(F'(u) F'(v))|| \le \omega_0 ||u v||$ for all $u, v \in D$;
- iii) $h_0 = \alpha \omega_0 \le \frac{1}{2};$
- iv) $\mathcal{B} = \bar{B}(u_0, \rho_0) \subset D$ for $\rho_0 = (1 \sqrt{1 2h_0})/\omega_0$, where B defines an open ball.

Then the Newton sequence from u_0 is well-defined and remains within the ball \mathcal{B} . A solution $u^* \in \mathcal{B}$ with $F(u^*) = 0$ exists, and the Newton sequence converges to it. Furthermore, if we define $\rho^+ = (1 + \sqrt{1 - 2h_0})/\omega_0$, then u^* is unique within $D \cap B(u_0, \rho^+)$.

One of the main features of this theorem is that all of its assumptions except for Lipschitz continuity are verified at the initial guess u_0 . Convergence can be assured a priori, without needing to assume the existence of a root beforehand.

Nevertheless, this theorem is not a suitable foundation for the purpose at hand. Suppose there exist u_1^* and u_2^* with $F(u_1^*) = F(u_2^*) = 0$ and $u_1^* \neq u_2^*$. Now consider an initial guess u_0 that provably converges to u_1^* by the Newton–Kantorovich theorem. The result is a ρ^+ such that $u_1^* \in B(u_0, \rho^+)$ and $u_2^* \notin B(u_0, \rho^+)$, Figure 3.2a. In order to prove convergence of the deflated function $M(u; u_1^*)F(u)$, we would need to establish a $\rho'^+ > \rho^+$ such that $u_2^* \in B(u_0, \rho'^+)$. However, this would imply that $u_1^* \in B(u_0, \rho'^+)$, Figure 3.2b. The assumptions of the Newton–Kantorovich theorem imply that the Fréchet derivative is invertible everywhere in the ball, but the Fréchet derivative of the deflated function is not defined at u_1^* , and hence the assumptions





- (a) Convergence before deflation
- (b) Convergence after deflation

Fig. 3.2: Sketch of why sufficient conditions for multiconvergence cannot be based on the Newton–Kantorovich theorem. The Newton–Kantorovich theorem describes a ball of convergence centred at the initial guess u_0 . In order to show convergence to multiple solutions u_1^* and u_2^* we need the convergence region to grow, i.e. $\rho'^+ > \rho^+$. This would imply that the deflated root lies within the new region of convergence, which poses regularity problems on the Fréchet derivative of the deflated function in the convergence region.

cannot hold after deflation. The same argument holds for the Newton-Mysovskikh theorem [22].

We therefore seek to base our analysis on results whose conditions are verified at the roots themselves, instead of at the initial guess. The theorem we will build upon is the Rall–Rheinboldt theorem [24, 26], again stated in affine-covariant form.

THEOREM 3.2 (Affine-covariant Rall-Rheinboldt [24, 26]). Let $F: D \to Y$ be a continuously Fréchet differentiable function on the open convex subset $D \subseteq U$. Suppose that there exists a $u^* \in D$ such that $F(u^*) = 0$, and suppose further that

- i) $F'(u^*)^{-1}$ exists;
- ii) $||F'(u^*)^{-1}(F'(u) F'(v))|| \le \omega^* ||u v||$ for all $u, v \in D$.

Then any $\rho^* \leq 2/(3\omega^*)$ such that $\mathcal{B} = B(u^*, \rho^*) \subset D$ has the property that starting at $u_0 \in \mathcal{B}$, the Newton sequence is well-defined and remains within \mathcal{B} . The Newton sequence converges to $u^* \in \mathcal{B}$. Furthermore, if we define $\rho^+ = 1/\omega^*$, then u^* is unique within $D \cap B(u^*, \rho^+)$.

A crucial ingredient of this theorem is the affine covariant Lipschitz continuity of the Fréchet derivative F'. Before extending this theorem to the deflated case, we first give a lemma regarding the product of Lipschitz continuous functions.

Lemma 3.3 (Product of Lipschitz continuous functions). Let X,Y and Z be Banach spaces and let L(Y,Z) be the vector space of bounded linear operators from Y to Z with induced operator norm. Let $F: X \to Y$ and $G: X \to L(Y,Z)$ be Lipschitz continuous functions on the open subset $D \subseteq X$ with Lipschitz constants ω_F and ω_G respectively. Assume further that F and G are bounded on D, i.e. there exist $N_F, N_G \in \mathbb{R}$ such that $\|F(x)\| < N_F$ and $\|G(x)\| < N_G$ for all $x \in D$. Then the product $GF: X \to Z$ is bounded and Lipschitz continuous on D with Lipschitz

constant $(N_F\omega_G + N_G\omega_F)$.

Proof. Let $x, y \in D$. As both F and G are bounded on D their product is bounded as well:

$$||G(x)F(x)|| \le ||G(x)|| ||F(x)|| \le N_G N_F < \infty.$$
 (3.1)

Furthermore,

$$||G(x)F(x) - G(y)F(y)|| = ||G(x)F(x) - G(x)F(y) + G(x)F(y) - G(y)F(y)||$$

$$\leq ||G(x)F(x) - G(x)F(y)|| + ||G(x)F(y) - G(y)F(y)||$$

$$\leq ||G(x)|| ||F(x) - F(y)|| + ||G(x) - G(y)|| ||F(y)||$$

$$\leq N_G ||F(x) - F(y)|| + N_F ||G(x) - G(y)||$$

$$\leq N_G \omega_F ||x - y|| + N_F \omega_G ||x - y||$$

$$= (N_F \omega_G + N_G \omega_F) ||x - y||,$$
(3.2)

which proves the claim. \square

We now consider the situation where one solution u_1^* is known and has been deflated. We state sufficient conditions on the original residual and deflation operator that guarantee convergence to another solution u_2^* .

Theorem 3.4. Let $F: D \to Y$ be a continuously Fréchet differentiable function on the open convex subset $D \subseteq U$. Suppose there exists $u_2^* \in D$ such that $F(u_2^*) = 0$. Further assume there exists $u_1^* \in D$, $u_1^* \neq u_2^*$, such that $F(u_1^*) = 0$. This solution is deflated with a deflation operator $M(\cdot; u_1^*) : D \setminus \{u_1^*\} \to GL(Y, Y)$. Suppose there exists an open bounded convex subset $E \subseteq D \setminus \{u_1^*\}$ with $u_2^* \in E$ such that the following conditions hold:

- i) $F'(u_2^*)^{-1}$ exists;
- ii) $||F'(u_2^*)^{-1}(F'(u) F'(v))|| \le \omega^* ||u v||$ for all $u, v \in E$;
- iii) $M(u; u_1^*)$ is continuously Fréchet differentiable for all $u \in E$;
- iv) $||M'(u; u_1^*) M'(v; u_1^*)|| < \omega_{M'} ||u v||$ for all $u, v \in E$.

Then there exists a $\rho > 0$ such that the Newton sequence from $u_0 \in \mathcal{B} = B(u_2^*, \rho)$ on the deflated function $M(u; u_1^*)F(u)$ is well-defined, remains in \mathcal{B} and converges to $u_2^* \in \mathcal{B}$.

If the norm on U is twice continuously differentiable on E, the deflation operator (1.6) satisfies these conditions. In this case, we can use the composition rule for differentiable functions to show that the deflation operator is in turn twice differentiable on E. This implies that the deflation operator is Lipschitz continuous, as E is bounded. For $2 \le p < \infty$, the L^p norm is at least twice continuously differentiable on any open subset not containing zero [28, Theorem 8]. More generally, if the Banach space U is isomorphic to a Hilbert space, then it can be equipped with twice differentiable norms [18, 11]. Thus, the conditions demanded are satisfied in typical cases of interest.

Proof. As F(u) and $M(u; u_1^*)$ are continuously Fréchet differentiable on E, they are Lipschitz continuous as well by boundedness of E. Lipschitz continuity implies that the operators are bounded on E and thus F(u), F'(u), $M(u; u_1^*)$ and $M'(u; u_1^*)$ are all bounded on E. As a result the Fréchet derivative of the deflated operator

$$(M(u; u_1^*)F(u))' = M(u; u_1^*)F'(u) + M'(u; u_1^*)F(u)$$
(3.3)

is Lipschitz continuous by use of the triangle inequality and Lemma 3.3.

Since u_2^* is a root of F, the Fréchet derivative of the deflated residual there is $M(u_2^*; u_1^*)F'(u_2^*)$. For any $u \in D$ the deflation operator $M(u; u_1^*) \in GL(Y, Y)$ and is thus invertible. The Fréchet derivative of the deflated residual is thus invertible at u_2^* with

$$\left(\left[M(u; u_1^*) F(u) \right]' \right)^{-1} \Big|_{u_2^*} = F'(u_2^*)^{-1} M(u_2^*; u_1^*)^{-1}. \tag{3.4}$$

Combining these facts, there exists an (affine covariant) $\tilde{\omega}_2 > 0$ such that

$$\left\| \left([M(u_2^*; u_1^*) F(u_2^*)]' \right)^{-1} [(M(u; u_1^*) F(u))' - (M(v; u_1^*) F(v))'] \right\| \le \tilde{\omega}_2 \|u - v\|, \quad (3.5)$$

for all $u, v \in E$. Hence the conditions of Theorem 3.2 are satisfied for both F(u) and $M(u; u_1^*)F(u)$, and it can be applied to prove the claim. \square

We are now in a position to state sufficient conditions for convergence to two solutions with deflation and Newton's method. The proof applies the previous theorem, Theorem 3.4, and the Rall–Rheinboldt theorem, Theorem 3.2.

THEOREM 3.5 (Deflated Rall-Rheinboldt [4]). Let $F: D \to Y$ be a continuously Fréchet differentiable function on an open subset $D \subseteq U$. Suppose there exist $u_1^*, u_2^* \in D$ such that $F(u_1^*) = F(u_2^*) = 0$, $u_1^* \neq u_2^*$. Let E_1 be an open bounded convex subset such that $E_1 \subset D \setminus \{u_2^*\}$ and $u_1^* \in E_1$. Furthermore let E_2 be an open bounded convex subset such that $E_2 \subset D \setminus \{u_1^*\}$ and $u_2^* \in E_2$. Let $M(\cdot; u_1^*) : D \setminus \{u_1^*\} \to GL(Y, Y)$ be a deflation operator such that the following conditions hold:

- i) $F'(u_1^*)^{-1}$ and $F'(u_2^*)^{-1}$ exist;
- ii) $||F'(u_1^*)^{-1}(F'(u) F'(v))|| \le \omega_1^* ||u v||$ for all $u, v \in E_1$;
- iii) $||F'(u_2^*)^{-1}(F'(u) F'(v))|| \le \omega_2^* ||u v|| \text{ for all } u, v \in E_2;$
- iv) $M(u; u_1^*)$ is continuously Fréchet differentiable for all $u \in E_2$;
- v) $||M'(u; u_1^*) M'(v; u_1^*)|| \le \omega_{M'} ||u v||$ for all $x, y \in E_2$.

Then there exists an $\tilde{\omega}_2 > 0$ such that for all $u, v \in E_2$ there holds

$$\left\| \left(\left[M(u_2^*; u_1^*) F(u_2^*) \right]' \right)^{-1} \left[\left(M(u; u_1^*) F(u) \right)' - \left(M(v; u_1^*) F(v) \right)' \right] \right\| \le \tilde{\omega}_2 \|u - v\|.$$
 (3.6)

If $||u_1^* - u_2^*|| < \rho_1 + \rho_2$ for some $\rho_1 \le 2/(3\omega_1^*)$ and $\rho_2 \le 2/(3\tilde{\omega}_2)$ such that we have $B_1 = B(u_1^*, \rho_1) \subset E_1$ and $B_2 = B(u_2^*, \rho_2) \subset E_2$, then the intersection $B_1 \cap B_2$ is nonempty. Starting from any $u_0 \in B_1 \cap B_2$, Newton's method will first converge to $u_1^* \in E_1$ and then after deflation with $M(\cdot; u_1^*)$ will converge to $u_2^* \in E_2$.

The argument of Theorems 3.4 and 3.5 can be applied again to derive sufficient conditions for a single initial guess to converge to three or more solutions.

A natural question to ask is if Algorithm 2.1 will recover the behaviour of switching continuation, i.e. if it will always discover connected branches for sufficiently small $\Delta \lambda$. This is discussed in the following corollary.

COROLLARY 3.6 (Connected roots). Let $f: D \times \mathbb{R} \to Y$ and suppose there exists a $\lambda_c \in \mathbb{R}$ such that $f(\cdot, \lambda): D \to Y$ is a continuously Fréchet differentiable

function on the open subset $D \subseteq U$ for $\lambda > \lambda_c$. Furthermore assume that there exists $u_1^*(\lambda), u_2^*(\lambda) \in D$ such that $f(u_1^*(\lambda), \lambda) = f(u_2^*(\lambda), \lambda) = 0$ and $u_1^*(\lambda) \neq u_2^*(\lambda)$ for $\lambda > \lambda_c$ and $u_1^*(\lambda_c) = u_2^*(\lambda_c)$. Assume that for fixed $\lambda > \lambda_c$ all conditions from Theorem 3.5 hold for the function $f(\cdot, \lambda) : D \to Y$ so that $\rho_1(\lambda), \rho_2(\lambda) \in \mathbb{R}$ as in Theorem 3.5 are well defined. If

$$\lim_{\lambda \downarrow \lambda_c} \frac{\|u_1^*(\lambda) - u_2^*(\lambda)\|}{\rho_1(\lambda) + \rho_2(\lambda)} < 1, \tag{3.7}$$

then an initial guess $u_0 \in D$ exists which converges to both u_1^* and u_2^* using Newton's method and deflation for λ sufficiently close to λ_c .

By assumption, $||u_1^*(\lambda) - u_2^*(\lambda)|| \to 0$ as $\lambda \downarrow \lambda_c$. As $\rho_1(\lambda) < ||u_1^*(\lambda) - u_2^*(\lambda)||$ (and similarly for $\rho_2(\lambda)$), $\rho_1(\lambda) + \rho_2(\lambda) \to 0$ also. Thus, the evaluation of the left-hand side of (3.7) requires the application of L'Hôpital's rule.

A similar formulation applies to the case of branches meeting as $\lambda \uparrow \lambda_c$, and to more than two roots. Our practical experience does indeed suggest that Algorithm 2.1 is always able to find branches connected via a bifurcation point; we conjecture that (3.7) always holds for sufficiently regular functions.

Note that these results are nonconstructive, i.e. the Lipschitz constants arising and the resulting radii of convergence are not in general known. Thus, it could be the case that the region of multiconvergence is too small to be of practical use in bifurcation analysis. We therefore apply Algorithm 2.1 to several problems of interest in the literature to investigate the robustness and efficiency of deflated continuation.

4. Examples.

4.1. Roots of unity. We consider the complex roots of unity

$$z^q - 1 = 0 \tag{4.1}$$

as the exponent q is varied. For $q \in \mathbb{N}_+$, the solutions are $\exp(2\pi i k/q)$ for $k = 1, \ldots, q$; this example studies how these solutions bifurcate for non-integer exponents.

Algorithm 2.1 was applied to (4.1) from q=2 to q=9 with $\Delta q=0.1$. Deflation was applied with power p=2 and shift $\sigma=1$. The resulting bifurcation diagram is shown in Figure 4.1, where the quantity plotted is the argument of the solution. For q=2, the solutions are $z=\pm 1$; the solution z=-1 bifurcates and the resulting solutions approach $z=\pm i$ as $q\to 4$. At q=4, z=-1 undergoes another bifurcation, and the process repeats. In general there is a bifurcation at z=-1 for $q\in 2\mathbb{N}_+$, and the resulting branches are mutually disconnected from each other.

As the bifurcation diagram is disconnected, switching continuation would identify at most one branch from any given initial solution. By contrast, deflated continuation identifies the new solutions at z=-1 immediately and correctly computes the entire diagram.

4.2. Deformation of a slender beam. The deformation of a slender vertical beam under loading is governed by Euler's elastica equation [19]

$$\theta'' + \lambda^2 \sin(\theta) = \mu, \qquad \theta(0) = \theta(1) = 0,$$
 (4.2)

where s is the arclength along the beam, $\theta(s)$ is the angle relative to the vertical axis, λ is the longitudinal force and μ is the transversal force. This system has long served as a model problem in bifurcation analysis [25].

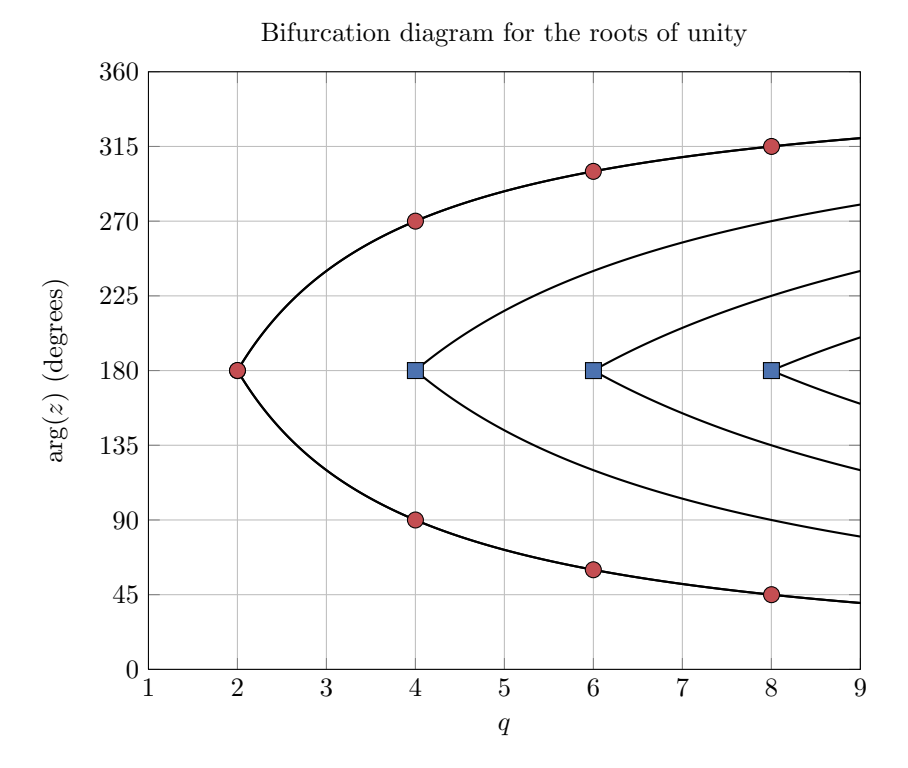


Fig. 4.1: Bifurcation diagram for the roots of unity (4.1) as a function of exponent q. The trivial branch z=1 is not shown. The bifurcation diagram is disconnected; switching continuation from q=2, z=-1 would only identify the branch marked with red circles. Blue squares denote the discovery of disconnected branches with deflation.

Algorithm 2.1 was applied to (4.2), from $\lambda = 0$ to $\lambda = 4\pi$, with continuation step $\Delta \lambda = 0.1$. The equation was discretized with 10^4 piecewise linear finite elements using FEniCS [20] and PETSc [3]. In the absence of a transversal force ($\mu = 0$), the initially straight solution $\theta(s) = 0$ forms a trivial branch and was thus deflated before beginning Algorithm 2.1. Newton's method was terminated with failure if convergence did not occur within 10^2 iterations. Deflation was applied with power p = 2, shift $\sigma = 1$ and with distances measured in the H^1 norm. After the forward continuation pass, arclength continuation backwards in λ was performed (without deflation) to complete the small sections of the bifurcation diagram where branches were not immediately discovered (cf. Figure 1.2b). The functional used was the L^2 norm, signed by $sign(\theta'(0))$.

A series of pitchfork bifurcations at $\lambda = n\pi$ for $n \in \mathbb{N}_+$ (corresponding to the eigenvalues of the associated linear problem) result in the buckled modes emanating from the trivial branch. As all branches meet at bifurcation points with the trivial branch, both switching continuation and deflated continuation compute the entire bifurcation diagram, Figure 4.2a. However, if a transversal force is applied ($\mu = 1/2$), the reflective symmetry is destroyed and the symmetric pitchfork bifurcations degenerate. In this case, the initial branch disconnects from all other branches, resulting

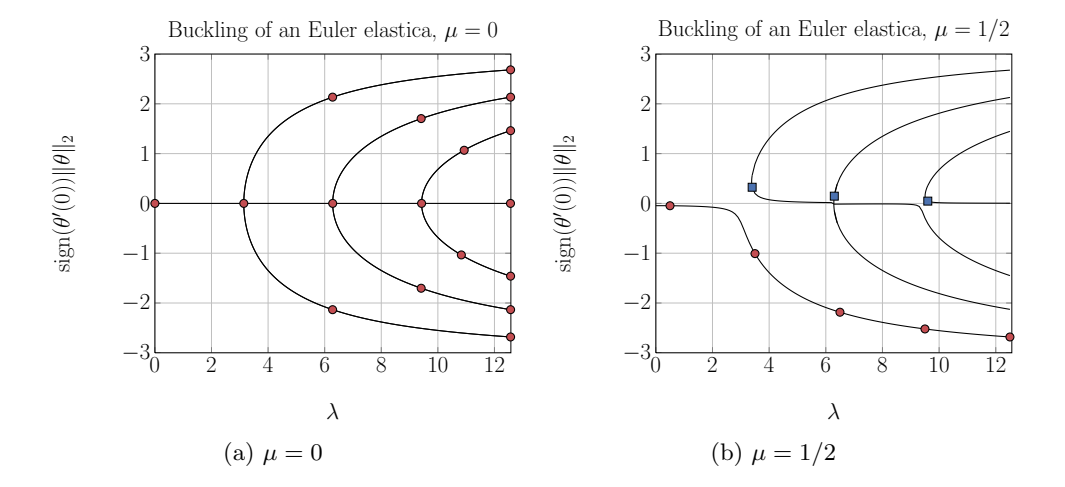


Fig. 4.2: Bifurcation diagrams for the Euler elastica equation (4.2) as a function of longitudinal loading λ , for $\mu = 0$ and $\mu = 1/2$. For $\mu = 0$, the bifurcation diagram is continuous and both switching continuation and deflated continuation discover the entire diagram. For $\mu = 1/2$, the bifurcation diagram is disconnected: switching continuation only discovers the part of the diagram labelled with red circles, whereas deflated continuation correctly computes the entire diagram. Blue squares denote the discovery of disconnected branches with deflation.

in a disconnected bifurcation diagram, Figure 4.2b. All of these other branches are missed with switching continuation applied to this path, yielding an incomplete representation of the dynamics of the system¹. Deflated continuation correctly computes the bifurcation diagram without continuation along multiple parameters.

4.3. Nonlinear pendulum. In the previous example, an additional source term destroyed the symmetry of the bifurcation diagram. This example serves to demonstrate that the same effect can be achieved by inhomogeneous boundary conditions. The angle of a pendulum to the vertical is described by the same equation,

$$\theta'' + \sin \theta = 0, \tag{4.3}$$

but here we impose inhomogeneous Dirichlet conditions $\theta(0) = \theta(10) = 2$. It is well known that with these boundary conditions this equation permits multiple solutions [5]. One possible way to compute these solutions is to attempt a homotopy from the linear equation $\theta'' = 0$ via the addition of a parameter ε multiplying the nonlinear term:

$$\theta'' + \varepsilon \sin \theta = 0, \qquad \theta(0) = \theta(10) = 2.$$
 (4.4)

For $\varepsilon = 0$, (4.4) reduces to a trivial linear problem; for $\varepsilon = 1$, the problem of interest is recovered. It is clear that homotopy methods based on switching continuation will

 $^{^1}$ It is possible to identify all of these solutions with switching continuation as follows: set $\mu=0$ and continue λ from 0 to 4π ; set $\lambda=4\pi$ and continue μ from 0 to 1/2; set $\mu=1/2$ and continue λ from 4π to 0. However, this is laborious and requires expert knowledge of the system; the right continuation strategy may not be obvious in more complex cases.

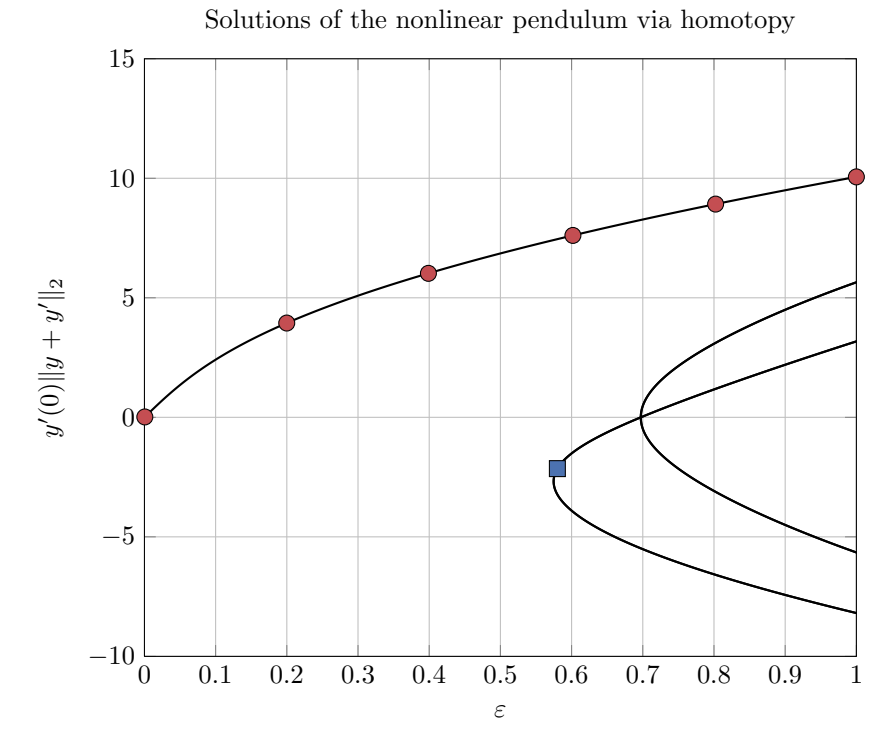


Fig. 4.3: Bifurcation diagram for the nonlinear pendulum (4.4) as a function of homotopy parameter ε . As before, switching continuation only discovers that part of the diagram labelled with red circles. The blue square denotes the discovery of a disconnected branch with deflation.

identify a solution for $\varepsilon = 1$ only if there is a branch that continuously connects it to the solution for $\varepsilon = 0$ [23, §11.3].²

Algorithm 2.1 was applied to (4.4), from $\varepsilon = 0$ to $\varepsilon = 1$, with continuation step $\Delta \varepsilon = 10^{-2}$. The equation was discretized with 10^4 standard piecewise linear finite elements using FEniCS and PETSc. The same deflation and solver settings were used as in the previous example. The functional considered was the product of the derivative at the left endpoint and the H^1 norm of the solution.

The resulting bifurcation diagram is shown in Figure 4.3. For $\varepsilon = 0$, the problem has a unique solution; as continuation is applied to this branch, no bifurcation points are encountered, and hence with switching continuation only one solution would be identified for $\varepsilon = 1$. As previously mentioned, a major difficulty with such homotopy methods is that the resulting bifurcation diagram must continuously connect the solution for $\varepsilon = 0$ to those of $\varepsilon = 1$; homotopy works robustly if this property holds, and fails if it does not. With deflated continuation, the requirements for success are weakened. Given a branch $\{(u(t), \lambda(t)) : t \in [0, 1]\}$, define its support to be

²Another approach would be to consider the associated initial-value problem with boundary conditions $\theta(0) = 2, \theta'(0) = \varepsilon$. The resulting IVP can be solved for varying values of ε and the solutions with $\theta(10) = 2$ selected. This shooting approach does not generalize to higher dimensions, and can be unstable.

 $\{\lambda(t): t \in [0,1]\} \subset \mathbb{R}$. Whereas switching continuation homotopy finds a solution only if there exists a continuously connected branch between it and the initial guess, deflated continuation homotopy only necessitates that the union of the supports of the branches covers the interval $[\lambda_{\min}, \lambda_{\max}]$. This is precisely the case in Figure 4.3. As the supports of the branches intersect, Algorithm 2.1 is able to discover the disconnected branches that come into existence at $\varepsilon \approx 0.575$ and $\varepsilon \approx 0.697$, and identifies four additional solutions that switching continuation homotopy neglects along this path.

4.4. Deformation of a hyperelastic beam. A major strength of deflated continuation is that it scales to fine discretizations of partial differential equations (PDEs). Unlike switching continuation, deflated continuation does not demand the nonscalable computation of determinants or difficult eigendecompositions to detect bifurcations or switch branches. In fact, all of the subproblems arising in deflated continuation can be solved efficiently if a good preconditioner is available for the underlying forward problem.

The example of section 4.2 modelled the deformation of a beam under compression with Euler's elastica equation. In this example, we model the same physical phenomenon, but with a two-dimensional compressible neo-Hookean hyperelastic PDE, solved with scalable Krylov methods and preconditioners. The potential energy Π is given by

$$\Pi(u) = \int_{\Omega} \psi(u) \, dx - \int_{\Omega} B \cdot u \, dx - \int_{\partial \Omega} T \cdot u \, ds, \qquad (4.5)$$

where Ω is the reference domain, $u:\Omega\to\mathbb{R}^2$ is the displacement, ψ is the elastic stored energy density, B is the body force per unit reference area, and T is the traction force per unit reference length. To define ψ , consider the deformation gradient

$$F = I + \nabla u, \tag{4.6}$$

the right Cauchy-Green tensor

$$C = F^T F, (4.7)$$

and its invariants $J = \det(C)$ and $I_c = \operatorname{tr}(C)$. The compressible neo-Hookean stored energy density is given by

$$\psi = \frac{\mu}{2}(I_c - 2) - \mu \log(J) + \frac{\lambda}{2}\log(J)^2, \tag{4.8}$$

where μ and λ are the Lamé parameters, which are calculated from the Young's modulus E and Poisson ratio ν . In this problem, we take $\Omega = (0,1) \times (0,0.1)$, B = (0,-1000), T = 0, $E = 10^6$, and $\nu = 0.3$. In addition, Dirichlet conditions are imposed on the left and right boundaries:

$$u(0,\cdot) = (0,0),\tag{4.9}$$

$$u(1,\cdot) = (0, -\varepsilon),\tag{4.10}$$

where ε is the parameter to be continued.

For a fixed ε , let $V_{\varepsilon} = \{u \in H^1(\Omega; \mathbb{R}^2) : u(0, \cdot) = (0, 0), u(1, \cdot) = (0, -\varepsilon)\}$ be the function space of admissible displacements. Minimizers of (4.5) are computed by seeking solutions of the associated optimality condition: find $u \in V_{\varepsilon}$ such that

$$\Pi'(u;v) = 0 \ \forall \ v \in V_0. \tag{4.11}$$

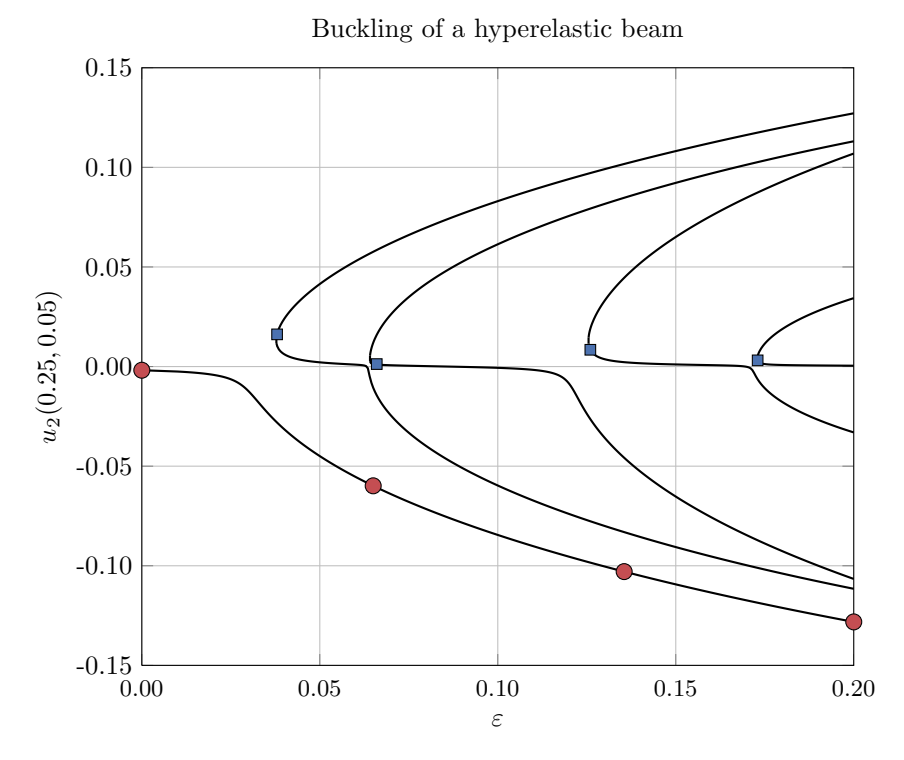


Fig. 4.4: Bifurcation diagram for the hyperelastic PDE formulation for the deformation of a beam (4.11) as a function of the displacement on the right-hand boundary. As before, switching continuation only discovers that part of the diagram labelled with red circles. Blue squares denote the discovery of disconnected branches with deflation.

Algorithm 2.1 was applied to (4.11), from $\varepsilon = 0$ to $\varepsilon = 0.2$, with continuation step $\Delta \varepsilon = 0.0005$. The equation was discretized with 2×10^4 piecewise linear finite elements using FEniCS and PETSc. Newton's method was terminated with failure if convergence did not occur within 10^2 iterations. Each Newton step was solved with the GAMG algebraic multigrid preconditioner [2], equipped with the near-nullspace of rigid body modes [12]. Deflation was applied with power p = 2, shift $\sigma = 1$ and with distances measured in the H^1 norm. The functional considered was the vertical component of displacement evaluated at (0.25, 0.05).

It is well-known that for B=T=0, (4.11) enjoys a \mathbb{Z}_2 reflective symmetry and its bifurcation diagram undergoes a series of pitchfork bifurcations as ε is increased, similar to Figure 4.2a. However, in this configuration the reflective symmetry has been broken by imposing a gravitational body force, causing the bifurcation diagram to disconnect. The resulting diagram is shown in Figure 4.4, and the computed solutions with positive functional value are shown in Figure 4.5. The bifurcation diagram has been computed correctly, indicating that Algorithm 2.1 is robust to the use of indirect solvers, and that it will scale to much finer discretizations of PDEs.

4.5. A generalized Bratu–Gelfand problem in two dimensions. Previous examples have demonstrated that deflated continuation is able to find branches that

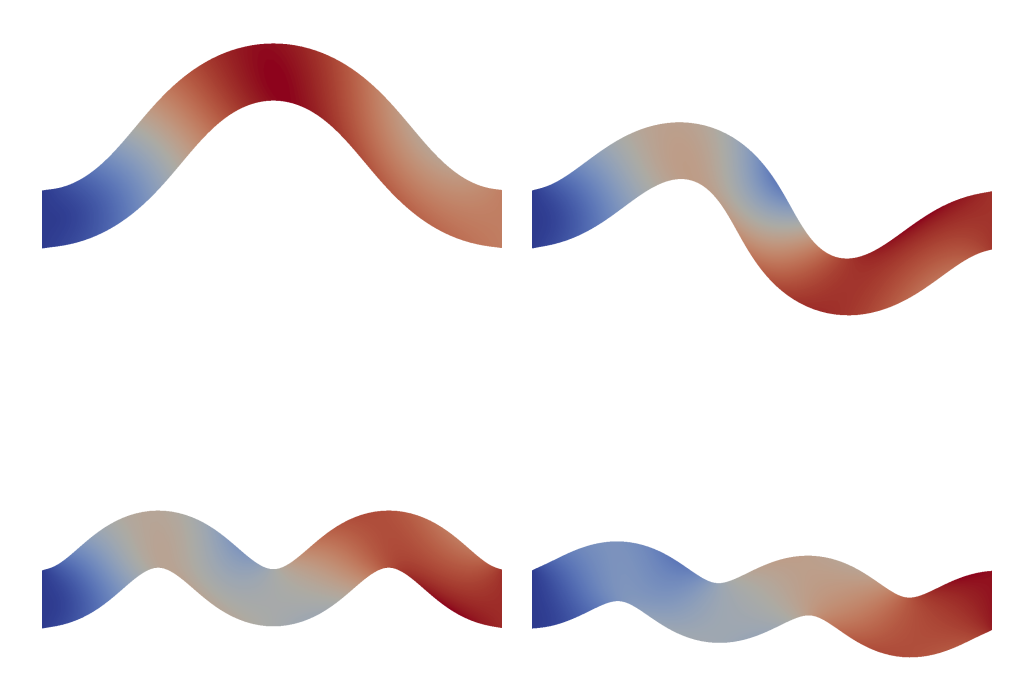


Fig. 4.5: Some of the solutions to the hyperelastic PDE (4.11) for $\varepsilon = 0.2$, found with deflated continuation. The color refers to the magnitude of the displacement from the reference configuration.

switching continuation misses because they are disconnected. Switching continuation can fail in other ways: for example, if a bifurcation is caused by an eigenvalue of even multiplicity crossing the origin, the standard bifurcation test functional (1.2) will neglect it. This example exhibits such a bifurcation, and demonstrates that deflated continuation is robust to this failure mode.

We consider the problem of Mittelmann [21]:

der the problem of Mittelmann [21]:

$$-\nabla^2 y = -10(y - \lambda e^y) \equiv \phi(y, \lambda), \quad \text{in } \Omega = (-0.5, 0.5)^2,$$

$$\nabla y \cdot \hat{n} = 0, \quad \text{on } \partial\Omega.$$
(4.12)

This is a generalization of the Bratu-Gelfand problem to multiple dimensions with the addition of a linear term, and has been used as a test problem for the PLTMG [21] and pde2path [29] continuation codes.

As noted by Mittelmann, this equation has two spatially constant solutions that satisfy $\phi(y,\lambda)=0$, i.e. $y(x)=\bar{y}$ with $\bar{y}=\lambda e^{\bar{y}}$. Linearising around \bar{y} with $y=\bar{y}+w$ yields an eigenvalue problem

$$\begin{split} -\nabla^2 w &= \left. \frac{\partial \phi}{\partial y} \right|_{(\bar{y},\lambda)} w = -10(1-\bar{y})w, &\quad \text{in } \Omega, \\ \nabla w \cdot \hat{n} &= 0, &\quad \text{on } \partial \Omega. \end{split} \tag{4.13}$$

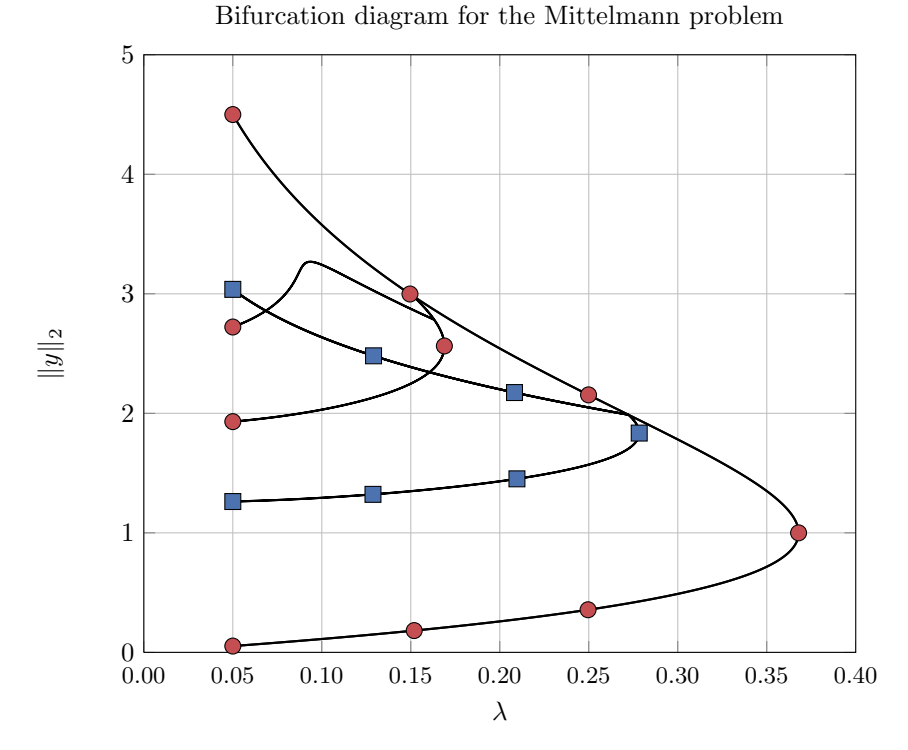


Fig. 4.6: Bifurcation diagram for the Mittelmann problem in two dimensions (4.12) as a function of λ . Standard switching continuation approaches that rely on the sign of the determinant (1.2) as a bifurcation test functional only discover that part of the diagram labelled with red circles. Blue squares denote the branch overlooked by switching continuation, but found by deflated continuation. Compare with [21, Figure 1], [29, Figure 2a].

Non-trivial perturbations of the constant solutions can be located by examining the eigenvalues and corresponding eigenfunctions of the Laplacian on Ω . The bifurcation points are found by solving $-10(1-\bar{y})=\mu_{m,n}$ where $\mu_{m,n}$ are the eigenvalues of the Laplacian with Neumann boundary conditions. In this case, $\mu_{m,n}=(m^2+n^2)\pi^2$ for $m,n\in\mathbb{N}_+$, and thus the bifurcations occur when $\bar{y}_{m,n}=1+\mu_{m,n}/10$ and $\lambda_{m,n}=\bar{y}_{m,n}e^{-\bar{y}_{m,n}}$. The initial bifurcation points occur at $\lambda_{0,0}=e^{-1}\approx 0.3678$ (a fold bifurcation), $\lambda_{0,1}=\lambda_{1,0}\approx 0.2724$ (a double pitchfork bifurcation), and $\lambda_{1,1}\approx 0.1519$ (a simple pitchfork bifurcation).

Consider again the computation of the bifurcation test functional τ , defined in (1.2). In the case when a simple bifurcation point is crossed τ will indicate this by negation, as one of the eigenvalues will have passed through the origin. On the other hand, if an eigenvalue of even multiplicity passes through the origin, τ remains unchanged. In this case the bifurcation point is overlooked, and the machinery of switching continuation is not activated.³

³Switching continuation can be rescued by deliberately breaking the symmetry of the domain, to unfold the double eigenvalues. Uecker et al. [29, Figure 4] suggest breaking the rotational symmetry of the domain by solving on $\tilde{\Omega} = (-0.5, 0.5) \times (-0.495, 0.495)$. The solutions found can then be continued

As the Mittelmann problem is two-dimensional, the Laplacian has degenerate eigenvalues of even multiplicity. For example, its eigenvalues $\mu_{0,1}$ and $\mu_{1,0}$ are identical but correspond to different eigenfunctions (related by rotation). Thus, the associated bifurcation point at $\lambda \approx 0.2724$ is missed by switching continuation, even though the bifurcation diagram is connected. This deficiency is not specific to this equation, and will manifest in any situation where such degeneracy of eigenvalues occurs.

By contrast, the specific nature of the bifurcation is irrelevant to deflated continuation; we expect the algorithm to find nearby solutions regardless of the details of how the branches are connected (or not connected). To investigate this, Algorithm 2.1 was applied to (4.12), for $\lambda \in [0.3678, 0.05]$, with continuation step $\Delta \lambda = -0.0001$. The equation was discretized with 1600 piecewise linear finite elements using FEniCS and PETSc. Newton's method was terminated with failure if convergence did not occur within 10^2 iterations. The same deflation and solver settings were used as in all previous examples. Following Uecker et al. [29], the functional considered was the L^2 norm of the solution.

The resulting diagram is shown in Figure 4.6. The outer branches (on the top and bottom) are the constant solutions, with branches bifurcating from the upper branch at $\lambda_{0,1} = \lambda_{1,0}$ and $\lambda_{1,1}$ as expected, and secondary bifurcations in turn emanating from these. Importantly, all branches in this interval have been discovered, including the branch overlooked with switching continuation (denoted with blue squares). Deflated continuation applies to both *connected* and disconnected bifurcation diagrams on which switching continuation fails.

5. Conclusion. We have presented a new algorithm for bifurcation analysis that relies on the elimination of known branches, rather than the detection and analysis of bifurcation points. In this way, the algorithm applies equally to connected and disconnected diagrams. We have developed an initial analysis of multiconvergence of Newton's method, giving sufficient conditions for when convergence to two solutions is guaranteed. In numerical experiments the algorithm is effective and succeeds where switching continuation fails.

Unlike switching continuation, the algorithm relies only on the solution of the original nonlinear problem with a fixed parameter value, and the solution of deflations of that problem. The latter is straightforward to implement and solve if a preconditioner for the former is available. There is no need to implement augmented systems for different kinds of bifurcation points, or to compute expensive test functionals, or to construct the nullspace of singular operators. Thus, if a scalable preconditioner for the undeflated Jacobian is available, it will be possible to apply the algorithm to massive discretizations of PDEs on supercomputers.

References.

- [1] J. P. Abbott, Numerical continuation methods for nonlinear equations and bifurcation problems, PhD thesis, Australian National University, 1977.
- [2] M. F. Adams, H. H. Bayraktar, T. M. Keaveny, and P. Papadopoulos, Ultrascalable implicit finite element analyses in solid mechanics with over a half a billion degrees of freedom, in ACM/IEEE Proceedings of SC2004: High Performance Networking and Computing, Pittsburgh, Pennsylvania, 2004.
- [3] S. Balay, S. Abhyankar, M. F. Adams, J. Brown, P. Brune, K. Buschelman, L. Dalcin, V. Eijkhout, W. D. Gropp, D. Kaushik,

to the true Ω . While this strategy is successful, it is laborious and requires expert knowledge of the system at hand.

- M. G. Knepley, L. Curfman McInnes, K. Rupp, B. F. Smith, and H. Zhang, *PETSc users manual*, Tech. Report ANL-95/11 Revision 3.6, Argonne National Laboratory, 2015.
- [4] C. H. L. BEENTJES, Computing Bifurcation Diagrams with Deflation, master's thesis, University of Oxford, 2015.
- [5] A. BIRKISSON, Numerical Solution of Nonlinear Boundary Value Problems for Ordinary Differential Equations in the Continuous Framework, PhD thesis, University of Oxford, 2014.
- [6] L. Blum, F. Cucker, M. Shub, and S. Smale, Complexity and Real Computation, Springer-Verlag, 1998.
- [7] K. M. BROWN AND W. B. GEARHART, Deflation techniques for the calculation of further solutions of a nonlinear system, Numerische Mathematik, 16 (1971), pp. 334–342.
- [8] K. A. CLIFFE, A. SPENCE, AND S. J. TAVENER, The numerical analysis of bifurcation problems with application to fluid mechanics, Acta Numerica, 9 (2000), pp. 39–131.
- [9] P. Deuflhard, Newton Methods for Nonlinear Problems, vol. 35 of Springer Series in Computational Mathematics, Springer-Verlag, 2011.
- [10] E. J. DOEDEL, AUTO: A program for the automatic bifurcation analysis of autonomous systems, in Congressum Numerantium: Proceedings of the 10th Manitoba conference on Numerical Mathematics and Computing, vol. 30, 1981, pp. 265–284.
- [11] M. Fabian, P. Habala, P. Hájek, V. Montesinos, and V. Zizler, Banach Space Theory: the Basis for Linear and Nonlinear Analysis, CMS Books in Mathematics, Springer-Verlag, 2011.
- [12] R. D. FALGOUT, An introduction to algebraic multigrid computing, Computing in Science & Engineering, 8 (2006), pp. 24–33.
- [13] P. E. FARRELL, Multiple local minima of PDE-constrained optimisation problems via deflation, 2015. arXiv:1508.07633 [math.OC].
- [14] P. E. FARRELL, Á. BIRKISSON, AND S. W. FUNKE, Deflation techniques for finding distinct solutions of nonlinear partial differential equations, SIAM Journal on Scientific Computing, 37 (2015), pp. A2026–A2045.
- [15] M. GOLUBITSKY AND D. SCHAEFFER, Singularities and Groups in Bifurcation Theory: Volume I, vol. 51 of Applied Mathematical Sciences, Springer, 1985.
- [16] L. Kantorovich, On Newton's method for functional equations, Doklady Akademii Nauk SSSR, 59 (1948), pp. 1237–1249.
- [17] H. B. Keller, Numerical solution of bifurcation and nonlinear eigenvalue problems, in Applications of Bifurcation Theory, P. H. Rabinowitz, ed., New York, 1977, Academic Press, pp. 359–384.
- [18] E. LEONARD AND K. SUNDARESAN, A note on smooth Banach spaces, Journal of Mathematical Analysis and Applications, 43 (1973), pp. 450–454.
- [19] R. LEVIEN, *The elastica: a mathematical history*, Tech. Report UCB/EECS-2008-103, University of California, Berkeley, 2008.
- [20] A. LOGG, K. A. MARDAL, G. N. WELLS, ET Al., Automated Solution of Differential Equations by the Finite Element Method, Springer, 2011.
- [21] H. D. MITTELMANN, Multilevel continuation techniques for nonlinear boundary value problems with parameter dependence, Applied Mathematics and Computation, 19 (1986), pp. 265–282.
- [22] I. Mysovskikh, On convergence of Newton's method, Trudy Matematicheskogo

- Instituta imeni V.A. Steklova, 28 (1949), pp. 145–147.
- [23] J. NOCEDAL AND S. J. WRIGHT, Numerical Optimization, Springer Verlag, 2006.
- [24] L. B. Rall, A note on the convergence of Newton's method, SIAM Journal on Numerical Analysis, 11 (1974), pp. 34–36.
- [25] E. L. Reiss, Column buckling an elementary example of bifurcation, in Bifurcation Theory and Nonlinear Eigenvalue Problems, J. B. Keller and S. Antman, eds., W. A. Benjamin, 1969, pp. 1–16.
- [26] W. C. Rheinboldt, An adaptive continuation process for solving systems of nonlinear equations, in Mathematical Models and Numerical Methods, vol. 3, Banach Center Publications, 1978, pp. 129–142.
- [27] R. SEYDEL, *Practical Bifurcation and Stability Analysis*, vol. 5 of Interdisciplinary Applied Mathematics, Springer, 3 ed., 2010.
- [28] K. Sundaresan, Smooth Banach spaces, Mathematische Annalen, 173 (1967), pp. 191–199.
- [29] H. UECKER, D. WETZEL, AND J. D. M. RADEMACHER, pde2path A Matlab package for continuation and bifurcation in 2D elliptic systems, Numerical Mathematics: Theory, Methods and Applications, 7 (2014), pp. 58–106.